Optics Letters

Extending the field of view by a scattering window in an I-COACH system

Mani Ratnam Rai,* A. Vijayakumar, and Joseph Rosen

Department of Electrical and Computer Engineering, Ben-Gurion University of the Negev, P.O. Box 653, Beer-Sheva 8410501, Israel
**Corresponding author: maniratnam1991@gmail.com*

Received 10 November 2017; revised 17 December 2017; accepted 10 January 2018; posted 24 January 2018 (Doc. ID 313283); published 22 February 2018

Interferenceless coded aperture correlation holography (I-COACH) is an incoherent digital holography technique developed to record and reconstruct 3D images of objects without two-wave interference. Herein, we introduce a novel technique to extend the field of view (FOV) of I-COACH beyond the limit imposed by the ratio between the finite area of the image sensor and the magnification of the optical system. Light diffracted from a point object located on the optical axis is modulated by a pseudorandom coded phase mask, and the central part of the point spread hologram (PSH) on the image sensor is recorded. The point object is shifted laterally to predetermined lateral locations in order to collect the exterior parts of the PSH. The recorded PSHs are stitched together to produce a synthetic PSH (SPSH) with an area nine times that of any individual PSH recorded by the image sensor. An object with a lateral extent beyond the FOV limit of the image sensor is placed at the same axial location as the point object, and the object hologram is recorded. The object is reconstructed by a cross-correlation between the zero-padded object hologram and the SPSH. Hence, the object parts beyond the FOV limit of the image sensor are recovered. An SPSH library is created for different axial planes, and the corresponding axial planes of the object are reconstructed.

OCIS codes: (090.1995) Digital holography; (110.0110) Imaging systems; (110.0180) Microscopy; (090.1760) Computer holography; (050.0050) Diffraction and gratings; (110.2945) Illumination design.

https://doi.org/10.1364/OL.43.001043

Digital holography is one of the fastest developing imaging technologies due to its inherent capability to record a 3D scene in a single exposure [1]. Many digital holography techniques are being developed to address various challenges in imaging. Numerous possibilities with digital holography techniques were found to unfold when incoherent light sources are used [2] instead of lasers. One important invention in this domain is the Fresnel incoherent correlation holography (FINCH) which defied the Lagrange invariant under special self-interference conditions and, thus, exhibited a lateral super-resolution [3,4]. Another self-interference incoherent digital holography technique called coded aperture correlation holography (COACH) was developed with imaging characteristics similar to that of a regular imaging system, but with the ability to record 3D information [5]. In COACH, the light diffracted from an object is modulated by a pseudorandom coded phase mask (CPM) and interfered with unmodulated light diffracted from the same object. Two holograms are recorded, one with a point object and another with the observed multi-point object. The image of the object is reconstructed by a cross-correlation between the two holograms. COACH has shown a high adaptability to bring forth advanced imaging characteristics such as 4D imaging with a wavelength as its fourth dimension [6] and improving the lateral image resolution by combining the concept of COACH and FINCH together [7]. Recently, it has been discovered that the 3D information of the object is present in both the amplitude, as well as the phase of the object wave modulated by the pseudorandom CPM. Therefore, two-wave interference is no longer necessary in COACH to record and reconstruct 3D information of the object [8]. This discovery simplified the optical configuration of COACH, and the stringent laboratory conditions necessary for an interferometer are no longer necessary. Several advancements in imaging technology have become possible using interferenceless COACH (I-COACH) [9,10].

In this Letter, we introduce a technique for extending the field of view (FOV) in I-COACH. The FOV of the investigated imaging systems is limited by the sensor area. Numerous techniques such as particle encoding [11], convolution techniques [12], and multiplexing of interferograms [13] are available to extend the FOVs of imaging systems. We present a technique implemented on the same I-COACH system [9,10] that involves the same process of acquiring two object holograms. The only modifications are a longer training stage of the system and a bit different reconstruction process. The technique can be generalized and applied to any imaging system.

The schematic of the I-COACH setup is shown in Fig. 1. The light from an incoherent source critically illuminates a point object located on the optical axis using a refractive lens L_1, whereas the light diffracted from the point object is collimated by a refractive lens L_2. A pseudorandom CPM is synthesized using the Gerchberg–Saxton algorithm (GSA) [9,14],

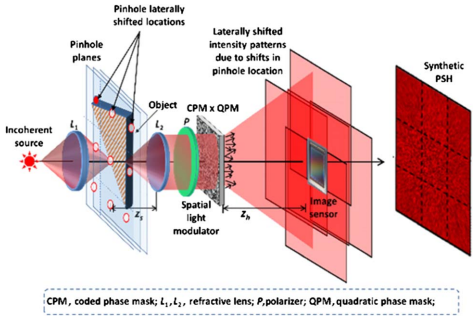

Fig. 1. Schematic of I-COACH for FOV extension. Only a single pinhole illuminates in any given time of the training stage.

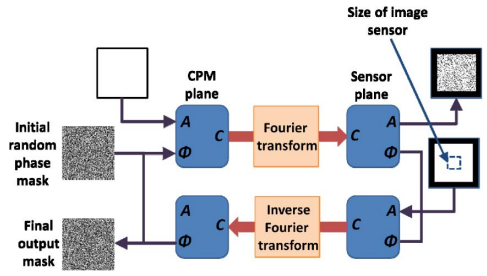

Fig. 2. GSA for synthesizing the two CPMs.

with a constraint to produce a uniform intensity pattern within a square dimensions of 3 × 3 larger than the area of the image sensor. The algorithm of GSA is shown in Fig. 2, and the computed CPM is displayed on a spatial light modulator (SLM). In order to satisfy the Fourier conditions of the GSA between the CPM and the sensor planes, a Fourier lens is necessary. Hence, the Fourier relation is satisfied by multiplying the CPM with a quadratic phase mask with a focal length equal to z_h, the distance between the SLM and the sensor plane. The light modulated by the CPM is incident on the image sensor, and the central part of the intensity pattern is recorded.

Before analyzing the proposed extended FOV system, let us summarize the analysis of regular I-COACH presented in our previous researches [8–10]. I-COACH is a linear space invariant system for 2D intensity functions. If the response for a δ function in the input is I_1, then for a 2D object, assumed as a collection of uncorrelated point objects $\sum_j a_j \delta(\bar{r}_s - \bar{r}_j)$, the response on the camera plane is $\sum_j a_j I_1(\bar{r}_o - M_T \bar{r}_j)$, where $M_T = z_h/z_s$ is the transverse magnification of the system, z_s is the distance between the object and lens L_2 and a_j are constants. The image of the object is reconstructed by cross-correlation between the object and the impulse responses. However, the cross-correlation between two positive functions introduces an unacceptable level of background noise. Therefore, both functions are converted to bi-polar functions by recording additional responses with another uncorrelated CPM and subtracting the two intensities for each case. In other words, the bi-polar point spread hologram (PSH) is $h = I_1 - I_2$, and the bi-polar object response is $\sum_j a_j [I_1(\bar{r}_o - M_T \bar{r}_j) - I_2(\bar{r}_o - M_T \bar{r}_j)] = \sum_j a_j h(\bar{r}_o - M_T \bar{r}_j)$, where I_2 is the impulse response with the second independent CPM. The image of the object is obtained as a cross-correlation between the bi-polar object response and the phase-only filtered version of the bi-polar PSH as the following:

$$\begin{aligned} P(\bar{r}_R) &= \iint \sum_j a_j h(\bar{r}_o - M_T \bar{r}_j) \tilde{h}^*(\bar{r}_o - \bar{r}_R) \mathrm{d}\bar{r}_0 \\ &= \mathfrak{F}^{-1}\left\{ \sum_j a_j |H| \exp(i\varphi - i2\pi M_T \bar{r}_j \cdot \bar{\rho}) \exp(-i\varphi) \right\} \\ &= \sum_j a_j \Lambda(\bar{r}_R - M_T \bar{r}_j) \approx o\left(\frac{\bar{r}_R}{M_T}\right), \end{aligned} \tag{1}$$

where $\mathfrak{F}\{\}$ stands for 2D Fourier transform. $\mathfrak{F}\{h\} = |H| \exp(i\varphi)$, $\mathfrak{F}\{\tilde{h}\} = \exp(i\varphi)$, and Λ is a δ-like function, approximately equal to 1 around (0,0) and to small negligible values elsewhere.

The FOV of regular I-COACH is limited by the size of the sensor area. For a sensor area of $D \times D$, the size of the FOV is $S \times S$ where $S = D/M_T$. In order to extend the FOV by a factor of 3 in the present case, we extend the training process of the system. Instead of measuring only the response of a single source point on the optical axis, we measure nine responses detected separately, each time for the input $\delta(x_s - Sk, y_s - Sl)$ where $k, l = -1, 0, 1$. Eight of the nine object points are located outside the FOV of the system, but part of each response is recorded by the camera. The recorded part can be expressed as $I_1(x_o - Dk, y_o - Dl)\mathrm{Rect}[(x_o, y_o)/D]$. Next, each recorded part is shifted to the location of its creating point, and all parts are summed to one synthetic three times larger impulse response as in the following:

$$\begin{aligned} \tilde{I}_1(x_o, y_o) = \sum_{k=-1}^{1} \sum_{l=-1}^{1} I_1(x_o - Dk, y_o - Dl) \mathrm{Rect}\left[\frac{(x_o, y_o)}{D}\right] \\ * \delta(x_o - Dk, y_o - Dl), \end{aligned} \tag{2}$$

where the symbol "*" represents a 2D convolution. To obtain a synthetic bi-polar PSH, the same process of recording the nine parts is repeated for the second independent CPM, and the final bi-polar PSH is $\tilde{h} = \tilde{I}_1 - \tilde{I}_2$. This relatively long training process is done only once and, when the training is completed, I-COACH operates as before [8–10] with an unlimited number of objects. An object located outside the original FOV of the system, around the point (kS, lS), can be expressed as $\sum_j a_j \delta(x_s - x_j + kS, y_s - y_j + lS)$, for $k, l = -1, 0, 1$ [but $(k, l) \neq (0, 0)$]. The recorded part of the response, at the limited area of the sensor, for the out-of-FOV object, minus the second camera shot with the second independent CPM, is given by

$$\begin{aligned} R(x_o, y_o) = \sum_j \tilde{h}(x_o - M_T x_j - Dk, y_o - M_T y_j - Dl) \\ \times \mathrm{Rect}\left[\frac{(x_o, y_o)}{D}\right]. \end{aligned} \tag{3}$$

The bi-polar object response is introduced into the center of the empty matrix of the size $3D \times 3D$ and correlated with the phase-only filtered version of the synthetic PSH (SPSH) as the following:

$$P(\bar{r}_R) = \iint \sum_j \bar{h}(x_o - M_T x_j - Dk, y_o - M_T y_j - Dl)\,\mathrm{Rect}\left[\frac{(x_o, y_o)}{D}\right] \times \bar{h}'^{*}(x_o - x_R, y_o - y_R)\,\mathrm{d}\bar{r}_0 = \sum_j a_j \Lambda(\bar{r}_R - M_T \bar{r}_j - D\bar{v}) \approx o\left(\frac{\bar{r}_R}{M_T} - D\bar{v}\right), \quad (4)$$

where $\bar{v} = (k, l)$. The reconstruction is achieved because at $(x_R, y_R) = (Dk, Dl)$ there is a high correlation between the recorded response of the object and the SPSH.

The cross-correlation reconstructs the object information in the axial plane of recording the PSH with a magnification of $M_T = z_h/z_s$. For 3D imaging, the PSH sets are recorded in a similar fashion along all the possible axial planes and compiled into a SPSH library. When a SPSH corresponding to an axial location is correlated with the object hologram, the corresponding object plane is reconstructed. The technique does not require any kind of special processing during the recording of the object holograms as in the case of other reported techniques [11–13]. The object hologram is recorded as previously [8–10], with only two camera shots and without any motion.

The experimental verification of the proposed FOV extension was carried out using a digital holography setup shown in Fig. 3. The experimental setup consists of two illumination channels with identical LEDs emitting light at a wavelength of 635 nm (Thorlabs LED635L, 170 mW, $\lambda = 635$ nm, $\Delta\lambda = 10$ nm). Two identical lenses, L_{1A} and L_{1B}, were used to critically illuminate three transparent digits "6,""0," and "1." In channel 1, the objects "1" and "6" are mounted outside the FOV of the imaging system whereas, in channel 2, the object "0" was mounted on the optical axis to be well within the FOV of the imaging system. The distance of the three objects from the refractive lens L_2 with a focal length of 17.5 cm is about 17.5 cm. The distance between the lens L_2 and the phase-only reflective SLM (Holoeye PLUTO, 1920 × 1080 pixels, 8 μm pixel pitch, phase-only modulation) is 20.5 cm. The distance between the lens L_2 and the center of beam splitter BS_2 is 15 cm. The distance between the SLM and the image sensor (Thorlabs 8051-M-USB, 3296 × 2472 pixels, 5.5 μm pixel pitch, monochrome) is $z_h = 40$ cm.

A central square of 11.4 × 11.4 mm from the image sensor participates in the experimental demonstration. The FOV in the object plane is reduced by limiting the sensor plane to only 3.8 × 3.8 mm, i.e., one-ninth of the above mentioned large square. Consequently, the FOV in the object plane is reduced to 1.7 × 1.7 mm. The pseudorandom CPMs displayed on the SLM are synthesized using the GSA to produce a uniform magnitude over the large square of 11.4 × 11.4 mm.

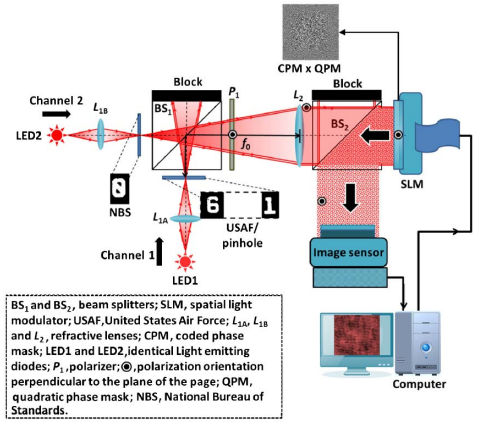

Fig. 3. Experimental setup of I-COACH with extended FOV.

In channel 1, a pinhole with a diameter of 80 μm is mounted on the optical axis at a distance of 17.5 cm from the lens L_2, and only the central section of the image sensor of 3.8 × 3.8 mm (out of 11.4 × 11.4 mm) is recorded. Two such intensity patterns are recorded using two different CPMs synthesized from different initial random phase masks. The pinhole is laterally shifted eight times in steps of 1.7 mm in order to shift the intensity response on the sensor plane, such that all the peripheral sections of the intensity are recorded from the central constricted area of the image sensor of 3.8 × 3.8 mm. The magnification of the system is $z_h/z_s = 2.28$; therefore, a shift of 1.7 mm in the object plane induces a shift of 3.8 mm at the sensor plane which is of course equal to the central constricted sensor area. All over, for the same two CPMs, nine times the intensity patterns are recorded for the various shifts of the pinhole of $k \cdot 1.7$ mm horizontally, and $l \cdot 1.7$ mm vertically, where $k, l = -1, 0, 1$. The nine intensity segments for each pinhole position are stitched to obtain the large synthetic intensity pattern. After stitching, the intensity patterns are subtracted from each other to yield bi-polar PSH with the size of 11.4 mm × 11.4 mm. The objects "1" and "6" are mounted in channel 1, and the object "0" is mounted in channel 2 at the same axial location as the pinhole. The two intensity patterns with the same two CPMs used for the PSHs are recorded and subtracted from each other to obtain the bi-polar object hologram of the size of 3.8 mm × 3.8 mm. For comparison purposes, the object hologram denoted as $H_{\mathrm{OBJ},l}$ with the size of 11.4 × 11.4 mm is also recorded without area constriction on the image sensor. The images of the PSH when the pinhole is on the optical axis, SPSH, large object hologram ($H_{\mathrm{OBJ},l}$) without the area limitation, and object hologram with the area limitation are shown in Figs. 4(a)–4(d), respectively.

Three cases of object reconstructions shown in Fig. 5 are compared (1) $H_{\mathrm{OBJ}} \otimes H'_{\mathrm{PSH}}$, (2) $H_{\mathrm{OBJ},l} \otimes H'_{\mathrm{SPSH}}$, and (3) $H_{\mathrm{OBJ}} \otimes H'_{\mathrm{SPSH}}$, where the symbol "⊗" represents a 2D correlation, and the apostrophe indicates that only the phase of each H is used in the Fourier plane. It can be noted that when the object hologram of Fig. 4(d) and the PSH of Fig. 4(a), both recorded by a limited FOV system, are cross-correlated, only the object "0" is reconstructed, while the objects "6" and "1" are lost. When the SPSH is cross-correlated with the full object hologram (11.4 mm × 11.4 mm), the objects "6" and "1" are reconstructed along with the object "0." In the case of the extended FOV procedure, when the SPSH is cross-correlated with the object hologram of Fig. 4(d), all the

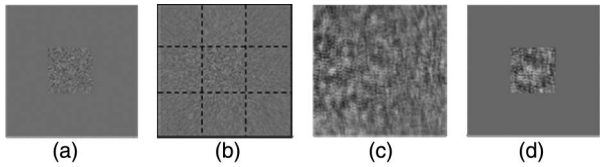

Fig. 4. Images of (a) PSH when the pinhole is on the optical axis, (b) SPSH, (c) large object hologram without the FOV limitation, and (d) object hologram with the limited FOV.

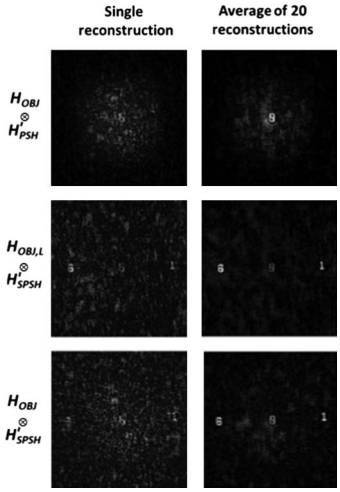

Fig. 5. Single and averaged reconstruction results of $H_{\mathrm{OBJ}} \otimes H'_{\mathrm{PSH}}$, $H_{\mathrm{OBJ,L}} \otimes H'_{\mathrm{SPSH}}$, and $H_{\mathrm{OBJ}} \otimes H'_{\mathrm{SPSH}}$.

objects "6," "0," and "1" are reconstructed, as in the previous case. To improve the signal-to-noise ratio of the reconstruction, multiple holograms of the pinhole and the object are recorded using CPMs synthesized from different initial random phase masks, and the complex reconstructions are averaged [15]. The averaged reconstructions are shown in the right column of Fig. 5. From the comparison between the lines of Fig. 5, it can be seen that by the use of the SPSH it is possible to image beyond the FOV limit imposed on the system by the limited area of the image sensor.

In the next experiment, the 3D imaging capabilities are demonstrated using a two-plane object constructed by mounting the objects in the channel 1 and 2 axially separated by a distance of 3 mm. Another SPSH is pre-recorded at the new location $z_{s1} = z_s - 3$ mm, with the pinhole and the same CPM sets, using the aforementioned stitching procedure. An object hologram is recorded with the constricted image sensor and zero padded. The recorded H_{SPSH} for each axial plane is cross-correlated with the H_{OBJ}, and the complex reconstructions are averaged over 20 different reconstructions. The reconstruction results for the two planes are shown in Fig. 6. As is expected, in Fig. 6(a) the digits "6" and "1" are in focus, whereas the digit "0" is out of focus, since the plane at z_{s1} is reconstructed. The reconstruction of the plane at z_s is shown in Fig. 6(b), where only the digit "0" is in focus.

In conclusion, we have proposed and demonstrated a novel technique for extending the FOV of a 3D imaging system which is limited by the finite area of the image sensor. In this technique, a SPSH is experimentally obtained by shifting the location of the point object and recording the different sections of a PSH followed by a stitching procedure. Even though the stitching process seems time-consuming, it should be noted that the procedure needs to be done only once along with the creation of the PSH library. Once the SPSH library is created, it can be used any number of times to perform 2D as well as 3D imaging with an extended FOV. The process of acquiring the object holograms and reconstructing the image are the same as in previous I-COACH demonstrations. The FOV extension procedure is not applied on an object under study,

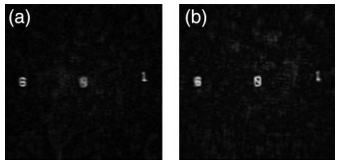

Fig. 6. Reconstruction results of the object using (a) SPSH of the plane of objects "6" and "1," and (b) SPSH of the plane of object "0."

but only on the PSH, and the imaging technique is free of interferometers or wave interference, as in the case of previously reported techniques [11–13].

The technique is demonstrated using a SPSH which is nine times that of the original PSH. However, the technique is not limited only to an enhancement of nine times. A higher FOV extension is possible by recording an additional number of PSH segments. The background noise associated with the reconstruction can be reduced by averaging over an additional number of complex reconstructions. The technique has been demonstrated on a I-COACH system. However, the location of the CPM inside the system is not essential. In principle, the CPM can be displayed as the input aperture of the system, as is demonstrated in [7]. Therefore, the CPM can be attached to many incoherent imaging systems. Extending the FOV of such systems can be achieved by the use of the training procedure of stitching the various impulse responses. Hence, we believe that the proposed technique is not limited only to I-COACH and can be easily adapted to other imaging and microscopy systems in which a wide FOV beyond the limit restricted by the size of the image sensor is necessary. In this technique, the FOV of I-COACH is extended at the expense of some reduction of the SNR which can be compensated by averaging over some number of reconstructed images. The overall result is FOV enhancement in exchange of some reduction of the time resolution.

Funding. Israel Science Foundation (ISF) (1669/16); Israel Ministry of Science and Technology (MOST).

REFERENCES

1. T.-C. Poon, *Digital Holography and Three-Dimensional Display* (Springer, 2007).
2. J. Rosen, G. Indebetouw, G. Brooker, and N. T. Shaked, J. Holography Speckle **5**, 124 (2009).
3. J. Rosen and G. Brooker, Opt. Lett. **32**, 912 (2007).
4. J. Rosen, N. Siegel, and G. Brooker, Opt. Express **19**, 26249 (2011).
5. A. Vijayakumar, Y. Kashter, R. Kelner, and J. Rosen, Opt. Express **24**, 12430 (2016).
6. A. Vijayakumar and J. Rosen, Opt. Lett. **42**, 947 (2017).
7. Y. Kashter, A. Vijayakumar, and J. Rosen, Optica **4**, 932 (2017).
8. A. Vijayakumar and J. Rosen, Opt. Express **25**, 13883 (2017).
9. M. R. Rai, A. Vijayakumar, and J. Rosen, Opt. Lett. **42**, 3992 (2017).
10. M. Kumar, A. Vijayakumar, and J. Rosen, Sci. Rep. **7**, 11555 (2017).
11. Z. Zalevsky, E. Gur, J. Garcia, V. Micó, and B. Javidi, Opt. Lett. **37**, 2766 (2012).
12. J.-C. Li, P. Tankam, Z.-J. Peng, and P. Picart, Opt. Lett. **34**, 572 (2009).
13. P. Girshovitz and N. T. Shaked, Light Sci. Appl. **3**, e151 (2014).
14. R. W. Gerchberg and W. O. Saxton, Optik **35**, 227 (1972).
15. A. Vijayakumar, Y. Kashter, R. Kelner, and J. Rosen, Appl. Opt. **56**, F67 (2017).